

Comparative Efficacy of Autologous Stromal Vascular Fraction and Autologous Adipose-Derived Mesenchymal Stem Cells Combined With Hyaluronic Acid for the Treatment of Sheep Osteoarthritis

Cell Transplantation
2018, Vol. 27(7) 1111–1125
© The Author(s) 2018
Article reuse guidelines:
sagepub.com/journals-permissions
DOI: 10.1177/0963689718773333
journals.sagepub.com/home/ct


Xiaoteng Lv^{1,*}, Jiyin He^{2,*}, Xue Zhang³, Xuan Luo¹, Na He¹,
Zhongwei Sun¹, Huitang Xia^{3,4,5}, Victor Liu¹, Li Zhang¹,
Xiangming Lin⁶, Liping Lin⁶, Huabin Yin⁶, Dong Jiang⁷, Wei Cao¹,
Richard Wang¹, Guangdong Zhou^{3,4,5,8}, and Wen Wang¹

Abstract

The current study explored whether intra-articular (IA) injection of autologous adipose mesenchymal stem cells (ASCs) combined with hyaluronic acid (HA) achieved better therapeutic efficacy than autologous stromal vascular fraction (SVF) combined with HA to prevent osteoarthritis (OA) progression and determined how long autologous ASCs combined with HA must remain in the joint to observe efficacy. OA models were established by performing anterior cruciate ligament transection (ACLT) and medial meniscectomy (MM). Autologous SVF (1×10^7 mononuclear cells), autologous low-dose ASCs (1×10^7), and autologous high-dose ASCs (5×10^7) combined with HA, and HA alone, or saline alone were injected into the OA model animals at 12 and 15 weeks after surgery, respectively. Compared with SVF+HA treatment, low-dose ASC+HA treatment yielded better magnetic resonance imaging (MRI) scores and macroscopic results, while the cartilage thickness of the tibial plateau did not differ between low, high ASC+HA and SVF+HA treatments detected by micro-computed tomography (μ CT). Immunohistochemistry revealed that high-dose ASC+HA treatment rescued hypertrophic chondrocytes expressing collagen X in the deep area of articular cartilage. Western blotting analysis indicated the high- and low-dose ASC+HA groups expressed more collagen X than did the SVF+HA group. Enzyme-linked immunosorbent assay showed treatment with both ASC+HA and SVF+HA resulted in differing anti-inflammatory and trophic effects. Moreover, superparamagnetic iron oxide particle (SPIO)-labeled autologous ASC signals were detected by MRI at 2 and 18 weeks post-injection and were found in the lateral meniscus at 2 weeks and in the marrow cavity of the femoral condyle at 18 weeks post-injection. Thus, IA injection of autologous ASC+HA may demonstrate better efficacy than autologous SVF+HA in blocking OA progression and promoting cartilage regeneration, and autologous ASCs (5×10^7 cells) combined with HA potentially survive for at least 18 weeks after IA injection.

¹ Cellular Biomedicine Group, Shanghai, China

² Department of Orthopaedics, Renji Hospital, Shanghai Jiao Tong University School of Medicine, Shanghai, China

³ Department of Plastic and Reconstructive Surgery, Shanghai 9th People's Hospital, Shanghai Jiao Tong University School of Medicine, Shanghai, China

⁴ Shanghai Key Laboratory of Tissue Engineering, Shanghai Jiao Tong University School of Medicine, Shanghai, China

⁵ National Tissue Engineering Center of China, Shanghai Jiao Tong University School of Medicine, Shanghai, China

⁶ Department of Radiology, Shanghai 5th People's Hospital, Fudan University, Shanghai 200240, China.

⁷ Department of Orthopaedics, Shanghai TCM-Integrated Hospital, Shanghai University of TCM, Shanghai 200082, China.

⁸ Research Institute of Plastic Surgery, Plastic Surgery Hospital, Weifang Medical College, Weifang 261041, Shandong, China

* Equal contributors

Submitted: April 10, 2017. Revised: March 15, 2018. Accepted: April 3, 2018.

Corresponding Author:

Wen Wang, Cellular Biomedicine Group, 333 Guiping Road, Shanghai 200233, China; Wen Wang, 19925 Stevens Creek Blvd, Suite 100, Cupertino, CA 95014, USA.

Email: ortho123@hotmail.com



Creative Commons Non Commercial CC BY-NC: This article is distributed under the terms of the Creative Commons Attribution-NonCommercial 4.0 License (<http://www.creativecommons.org/licenses/by-nc/4.0/>) which permits non-commercial use, reproduction and distribution of the work without further permission provided the original work is attributed as specified on the SAGE and Open Access pages (<https://us.sagepub.com/en-us/nam/open-access-at-sage>).

Keywords

autologous adipose-derived mesenchymal stem cells, autologous stromal vascular fraction, hyaluronic acid, osteoarthritis, superparamagnetic iron oxide, sheep model

Introduction

Osteoarthritis (OA) is the most prevalent and debilitating musculoskeletal disorder and is characterized by micro- and macro-injury-induced cell stress and extracellular matrix degradation that activates maladaptive repair responses, including pro-inflammatory innate immunity pathways¹. As an organ disease, the pathological changes induced by OA include cartilage degradation, subchondral bone sclerosis, ligament retrogression, synovium hyperplasia, and joint capsule hypertrophy². However, current existing therapies for OA primarily consist of symptom-modifying drugs in combination with nonsteroidal anti-inflammatory drugs (NSAIDs)³ and/or joint lubricants such as hyaluronic acid (HA)⁴ to reduce the wear and tear on joints, merely providing symptomatic relief from pain while failing to prevent 'joint failure' and regenerate damaged joint tissues^{2,5}. However, recently developed regenerative therapies employing mesenchymal stem cells (MSCs) or stromal vascular fraction (SVF) have shed light on clinical treatments for OA, providing substantial evidence in favor of cartilage regeneration and immunoregulation^{6–10}.

In 2011, autologous SVF, which comprises the heterogeneous cell populations released after the enzyme hydrolysis of adipose tissue, including adipose stromal cells, hematopoietic stem cells, endothelial cells, fibroblasts, lymphocytes, erythrocytes, monocyte/macrophages, and pericytes^{11–14}, was first applied in OA patients in combination with HA to induce cartilage regeneration; clinically, this treatment resulted in an alleviated visual analog score (VAS), improved range of motion, and magnetic resonance imaging (MRI) evidence of cartilage regeneration at 3-month follow up⁶. Since then, multiple clinical studies have demonstrated the efficacy of SVF for the treatment of OA. In 2013, a case series was reported in which autologous SVF with autologous platelet-rich plasma (PRP) was injected to treat 18 OA patients after arthroscopic debridement and lavage, and improved Western Ontario and McMaster Universities osteoarthritis index (WOMAC) scores, Lysholm knee scoring scales, VAS scores, and MRI evaluations were achieved⁷. Another study also demonstrated significant improvements in VAS scores, the knee injury and osteoarthritis outcome score (KOOS), and a second-look arthroscopic evaluation in 21 OA patients after treatment with autologous SVF with PRP compared with PRP alone in 23 OA patients⁸. Taken together, these data suggest SVF may represent a potentially effective therapeutic approach for the treatment of OA.

Adipose mesenchymal stem cells (ASCs) have also been widely investigated both preclinically and clinically for the treatment of OA^{9,15} because ASCs have advantages in terms

of their cell source as well as lower immunogenicity and stronger immunoregulatory ability compared with bone marrow-derived MSCs (BM-MSCs)^{16,17}. Our group recently observed that xenogeneic human ASCs engrafted into rabbit articular cartilage after 4 to 10 weeks of intra-articular (IA) injections promoted articular cartilage regeneration in a rabbit OA model¹⁸. Furthermore, we investigated the *in vivo* biodistribution of labeled-xenogeneic human ASCs in an immunocompetent rat OA model and observed the proliferation of engrafted human cells within the injected joint for approximately 10 weeks, indicating a correlation between cell therapy efficacy and a physical presence¹⁹. However, to the best of our knowledge, there is no direct evidence comparing the efficacy of autologous SVF and autologous ASCs for the treatment of OA in a large animal model that is similar to humans²⁰. Thus, it is important to understand whether the IA injection of autologous ASCs achieves better therapeutic efficacy than autologous SVF for preventing OA progression and to determine how long autologous ASCs must remain in the joint to observe efficacy (that is, the persistence of autologous stem cell therapy).

To address these important questions, we isolated and administered sheep adipose-derived autologous ASCs and autologous SVF in combination with HA into OA knees to determine whether autologous ASCs combined with HA are more effective in blocking OA progression compared with autologous SVF combined with HA in a standard large animal model. In addition, to evaluate the correlation between autologous ASC persistence and efficacy, ASCs were labeled with superparamagnetic iron oxide particles (SPIOs) and injected into OA knee joints in combination with HA for longitudinal detection by MRI.

Materials and Methods

Study Design and Animal Model

A total of 34 male small tail Han sheep (Jiagan Biotech, Shanghai, China), approximately 6 months old, skeletal immature, with a mean weight of 30 ± 5 kg, were used in this study. Among them, 4 sheep were set aside for the *in vivo* tracking study, while the other 30 sheep were randomly allocated to the following five treatment groups: Saline group (treated with 5 ml of normal saline, $n=6$); HA group (treated with 2.5 ml of saline + 2.5 ml of HA, $n=6$); ASC low-dose group (treated with 1×10^7 ASCs/2.5 ml of saline + 2.5 ml of HA, $n=6$); ASC high-dose group (treated with 5×10^7 ASCs/2.5 ml of saline + 2.5 ml of HA, $n=6$); and SVF group (treated with SVF containing 1×10^7 mononuclear cells/2.5 ml of saline + 2.5 ml of HA, $n=6$). A medium molecular weight (600–1500 kDa) of 2.5 mg/ml HA

Table 1. Group design and interventions.

Group	1st treatment (12 wk)	2nd treatment (15 wk)
Saline (n=6)	5 ml 0.9% normal saline	5 ml 0.9% normal saline
HA (n=6)	2.5 ml 0.9% normal saline + 2.5 ml HA	2.5 ml 0.9% normal saline + 2.5 ml HA
Low (n=6)	1 × 10 ⁷ ASCs/2.5 ml saline + 2.5 ml HA	1 × 10 ⁷ ASCs/2.5 ml saline + 2.5 ml HA
High (n=6)	5 × 10 ⁷ ASCs/2.5 ml saline + 2.5 ml HA	5 × 10 ⁷ ASCs/2.5 ml saline + 2.5 ml HA
SVF (n=6)	1 × 10 ⁷ SVF/2.5 ml saline + 2.5 ml HA	1 × 10 ⁷ SVF/2.5 ml saline + 2.5 ml HA
Tracing (n=4)	5 × 10 ⁷ SPIO-ASCs/2.5 ml saline + 2.5 ml HA	/

ASC: adipose mesenchymal stem cell; HA: hyaluronic acid; SPIO: superparamagnetic iron oxide particle; SVF: stromal vascular fraction.

(Jingfeng Pharmaceuticals, Shanghai, China) was used in the study. Grouping details and corresponding treatments are described in Table 1. Anterior cruciate ligament transection (ACLT) and medial meniscectomy (MM) of the right knee were performed according to previously described methods²¹. The non-surgery healthy knee joints were used as 'non-injured' group. After surgery, all sheep were permitted to exercise freely during daily life to ensure the occurrence of OA. At 7 weeks after knee surgery, each sheep underwent a second surgery to isolate adipose tissues from the cervicothoracic region for the generation of autologous SVF or ASCs. At 12 weeks after ACLT and MM, fresh ASCs and SVF were harvested to treat OA sheep according to their grouping, respectively. At 15 weeks, cryopreserved ASCs and SVF were used as a second dose. At 27 weeks after ACLT and MM (3 months after the second injection), all sheep were euthanized, and the knee joints were evaluated by performing imaging and histological analyses. For the tracking study (n=4), 5 × 10⁷ SPIO-labeled ASCs were injected into each sheep to track cell signals by performing MRI. The sheep were euthanized at week 14 or week 30 (Fig. 1). All animal protocols were approved by the Ethics Committee of Shanghai Jiao Tong University School of Medicine, and all subsequent experiments were performed in accordance with relevant guidelines and regulations²².

Isolation of SVF and ASCs

Adipose tissue (24.02 ± 9.31 g) was collected from each sheep at 7 weeks after ACLT and MM surgery to harvest autologous SVF or ASCs as previously described^{23,24}. Briefly, adipose tissues were first washed three times in phosphate-buffered saline (PBS) to remove red blood cells and tissue debris; then, fat was digested with 0.2% collagenases IV (Sigma C5138) (Sigma-Aldrich, St. Louis, MO, USA) at 37°C for 1.5 h. SVF pellets were obtained by centrifugation at 425 g for 5 min, followed by resuspension. The average yield of SVF was 1.88 × 10⁶ mononuclear cells

per 1 g of sheep adipose tissue. To obtain autologous ASCs, SVF pellets containing 1 × 10⁷ nucleated cells were cultured in 175 cm² flask in Dulbecco's modified Eagle's medium (Sigma-Aldrich) with 10% fetal bovine serum (Thermo Fisher Scientific, Waltham, MA, USA) at 37°C with 5% CO₂. After 24 h, non-adherent cells were removed, and the culture medium was replaced every 3 days. After 80–90% confluence, cells were collected as passage 0 ASCs. ASCs harvested at passage 4 were utilized. ASCs were characterized by performing flow analysis for the markers CD31 (1:50), CD44 (1:50) and CD45 (1:50) (BD Pharmingen, San Diego, CA, USA). ASC stemness was validated based on chondrogenic, osteogenic, and adipogenic differentiation verified by Alcian Blue, Alizarin Red, and Oil Red O staining (Merck Millipore, Darmstadt, Germany), respectively, according to the previous investigation²⁵. Briefly, for adipogenic and osteogenic differentiations, cells were seeded and grown in StemPro[®] adipogenesis and osteogenesis differentiation medium (Gibco, Carlsbad, USA) for 3 weeks, respectively. For chondrogenic differentiation, micromass culture was used and cells were cultured in StemPro[®] chondrogenesis differentiation medium (Gibco) for 4 weeks.

MRI Analysis for Therapeutic Efficacy

To evaluate the therapeutic efficacy of joint tissues, three sheep from each group were randomly selected for MRI using a 3.0 T MR System (MAGNETOM Skyra, Siemens, Germany) pre-operatively as well as 12 weeks and 27 weeks after surgery. All analyses were performed by three blinded experts (Drs XL, LL, and HY) using the magnetic resonance observation of cartilage repair tissue (MOCART) scoring system with sagittal T1-FSE (TR, 380 ms; TE, 25.4 ms; matrix, 512 × 512; flip angle, 90°; slice thickness, 3 mm; spacing between slices, 3.3 mm), sagittal FS-PD (2020/33/512 × 512/90°/3/3.3), sagittal STIR (5000/57.5/512 × 512/90°/3/3.3), coronal STIR (4200/58.9/512 × 512/90°/3/3.3), and axial FS-T2 (2900/59.2/512 × 512/90°/4/4.5) sequences, as previously described²⁶.

Macroscopic Evaluation and μ CT Analysis

In each group, femoral condyles of three randomly selected sheep were macroscopically evaluated according to the International Cartilage Research Society (ICRS) scores for cartilage repair^{27,28}. ICRS is a 3-point scoring system, each part being assigned a score between 0 and 4, giving an index with a range of 0 to 12 points (normal, 12; nearly normal, 11–8; abnormal, 7–4; and severely abnormal, 3–0). For μ CT analysis (Scanco μ CT40, Switzerland), all tibia samples were incubated for 15 minutes in 50 ml 20% Cysto Conray II/80% PBS at 37°C, and evaluated in an animal bed, providing a voxel size of 45 μ m, and scanned at 70 kVp, 114 μ A, 200 ms integration time, and 15–30 minutes acquisition time. In order to accurately segment the tibia articular cartilage from the subchondral bone, contour lines for the

articular cartilage and subchondral bone were manually drawn, and semi-automatic contouring was applied every 3–10 slices. The lower threshold was 30 HU (Hounsfield Unit), the upper threshold was 1000 HU (Gauss filter parameters: sigma=1.2, support=2) to segment cartilage from bone tissue according to the histogram analysis of the tissues. Direct distance transformation algorithms were used to quantify the average cartilage thickness from the bird's-eye view²⁹. All macroscopic and μ CT evaluations were performed by three blinded experts (Drs JH, HX, and DJ).

Histological and Immunohistochemical Analysis

Femoral condyle samples were collected and fixed in 4% paraformaldehyde for one week, followed by decalcification in ethylenediaminetetraacetic acid (EDTA)-buffered saline solution (pH 7.4, 0.25 mol/l) for 3 months at room temperature. Samples were then dehydrated via serial ethanol washing and embedded in paraffin for sectioning (6 μ m for each section). To assess the general morphology of the articular cartilage samples, sections obtained from sheep in each group underwent histological staining, including H&E (hematoxylin & eosin) staining and safranin-O and fast green staining (Sigma-Aldrich). Cartilage thickness was quantitatively assessed by three blinded experts (Drs JH, HX, and DJ), according to previously described methods³⁰. To identify hypertrophic chondrocytes in the cartilage, immunohistochemical staining using polyclonal rabbit anti-sheep collagen X antibodies (1:200) (GeneTex, Irvine, CA, USA) was performed.

Detection of Cytokines in Synovial Fluid

To determine whether levels of inflammatory cytokines and growth factors in knee joints changed after treatment, 1.5 ml of synovial fluid was collected from each knee joint at 27 weeks after surgery. Inflammatory cytokines, including interleukin (IL)-1 β , IL-6, and IL-10, growth factors including transforming growth factor (TGF)- β 1 and insulin-like growth factor (IGF)-1, and the chemokine stromal cell-derived factor (SDF)-1 α were detected with commercial enzyme-linked immunosorbent assay (ELISA) kits (RayBiotech, Norcross GA, USA) according to the manufacturer's instructions.

Immunoblot Analysis

To detect type X collagen protein levels, protein was extracted from cartilage samples at 27 weeks after euthanasia. Collagen X expression was detected using a standard immunoblot technique. Polyclonal rabbit anti-sheep collagen X antibodies (1:300) (GeneTex) and polyclonal rabbit glyceraldehyde-3-phosphate dehydrogenase (GAPDH) antibodies (1:1000) (Cell Signaling Technology, Beverly, MA, USA) were applied. Detection was performed using an enhanced chemiluminescence detection kit (Thermo Fisher

Scientific). The intensity of each band was normalized to GAPDH.

Autologous ASC Labeling and Longitudinal MRI Tracing

A total of 5×10^7 autologous ASCs at passage 4 were isolated from four individual sheep and labeled with SPIO (Biopal, Worcester, USA) according to the manufacturer's instructions. The SPIO-labeled autologous ASCs were then delivered into the OA knee joint of each sheep 12 weeks after ACLT. SPIO signals were tracked non-invasively using a 3.0 T MR imaging system (MAGNETOM Skyra, Siemens, Germany) under T2* sequence conditions (TR, 445 ms; TE, 4.36 ms; FOV, 159 mm; matrix, 384 \times 384; flip angle, 60°; slice thickness, 3 mm; spacing between slices, 3.6 mm) at 0 (12 weeks post-surgery), 6 (18 weeks post-surgery), 12 (24 weeks post-surgery), and 18 weeks (30 weeks post-surgery) after IA delivery of cells. Prussian blue staining was used to identify SPIO particles in articular cartilage sections. In order to exclude the possibility that SPIO positive cells were not the macrophages which swallowed labeled SPIO particles by phagocytosis, CD68 immunohistochemistry was also performed using mouse polyclonal anti-sheep CD68 antibody (Santa Cruz, 1:100).

Statistical Analysis

The data are expressed as the mean \pm SE. Differences among groups were tested for statistical significance by performing Kruskal–Wallis test followed by Dunn's post-test. *P*-values less than 0.05 were considered statistically significant.

Results

Autologous ASCs+HA Demonstrated Better Efficacy than SVF+HA for the Treatment of OA

At 12 weeks after ACLT and MM, MRI showed an absence of the anterior cruciate ligament and medial meniscus, fuzziness of the articular cartilage contour, effusion of the articular cavity, and bone marrow edema, indicating OA was successfully induced (Fig. 2A). At 27 weeks after ACLT and MM (12 weeks after the second injection), the autologous ASC+HA and SVF+HA groups all exhibited a more glossy, continuous, and intact layer of articular cartilage than the HA alone and saline alone groups (Fig. 2A). In particular, effusion of the articular cavity and defects in the cartilage and subchondral bone were obvious in both the HA alone and saline alone groups, demonstrating the efficacy of autologous ASC+HA and SVF+HA therapy. MOCART scores, which were evaluated by three independent observers, demonstrated the significantly increased efficacy of the low-dose ASC+HA treatment compared with the SVF+HA, HA alone, and saline alone groups (Fig. 2B).

Macroscopic evaluations of the articular surface of the femoral condyles in each group were performed by three

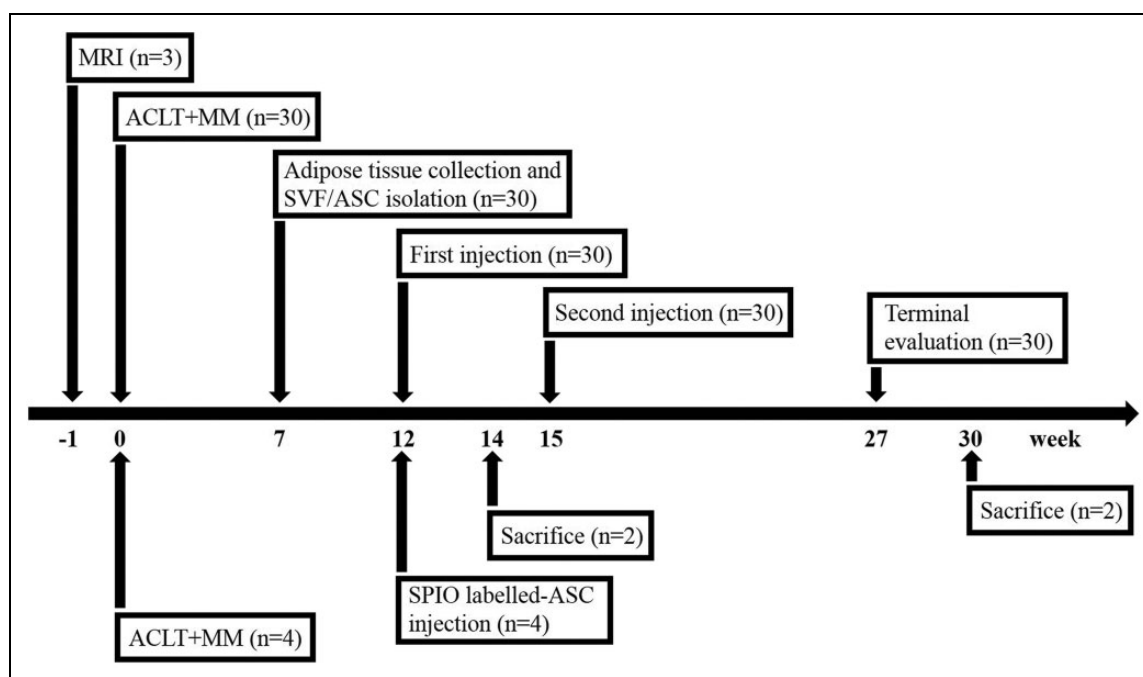


Fig. 1. Schedule and design of the study. At 1 day before surgery, three sheep were randomly selected to perform baseline MRI. In total, 34 sheep were performed ACLT+MM in which 30 sheep were divided into saline, HA, low ASC+HA, high ASC+HA, and SVF+HA groups, and 7 weeks later another operation took place to isolate adipose tissue manufacturing SVF and ASCs. At 12 and 15 weeks after surgery, each group was treated by different interventions. 30 sheep were sacrificed at week 27 after surgery. The remaining four sheep were used in the tracking study with SPIO-labeled ASC injection at week 12 and sacrificed at week 14 and week 30, respectively.

ACLT: anterior cruciate ligament transection; ASC: adipose mesenchymal stem cell; HA: hyaluronic acid; MM: medial meniscectomy; MRI: magnetic resonance imaging; SPIO: superparamagnetic iron oxide particle; SVF: stromal vascular fraction.

independent observers, and ulcerations in the articular cartilage were evident in the saline alone and HA alone groups, although HA treatment showed better efficacy than that of the saline group, whereas cartilage ulceration was alleviated with the autologous ASC+HA and SVF+HA treatments (Fig. 3A). Low-dose ASC+HA treatment (1×10^7 cells) resulted in a smoother and more continuous cartilage surface compared with SVF+HA treatment (1×10^7 cells): obvious ulcerations were observed in the trochlear groove area in three of six sheep in the SVF+HA group, while high-dose ASC+HA treatment (5×10^7 cells) yielded an even more continuous and intact articular surface than did the low-dose ASC+HA and SVF+HA treatments (Fig. 3A). Similarly, μ CT evaluations of the tibia plateau revealed a continuous and intact cartilage layer with no obvious cartilage destruction in the autologous high-dose and low-dose ASC+HA treatment groups, whereas visible structural changes and cartilage damage were observed in the saline, HA, and SVF+HA groups although there were no significant differences in the average cartilage thickness of tibial plateau among ASC+HA, SVF+HA, and HA alone groups (Fig. 3B and D). The low-dose ASC+HA treatment group had significantly higher ICRS scores compared with the saline and HA groups; however, the SVF+HA and high-dose ASC+HA groups had no significance of ICRS scores compared with the saline and HA groups. (Fig. 3C). Thus, IA

injection of autologous ASCs+HA and SVF+HA efficiently blocked OA pathogenesis and achieved superior therapeutic efficacy compared with that observed in the HA and saline groups. However, ASC+HA had better efficacy than SVF+HA for the treatment of OA when considering the ICRS score of the femoral condyle.

Histological Analysis revealed Good Cartilage Quality following the Autologous ASC+HA and SVF+HA Treatments

Histological results for both H&E staining (Fig. 4A) and safranin-O/fast green staining (Fig. 4B) of the medial epicondyle of the femur further revealed typical, homogenous articular cartilage structures with smooth, continuous surfaces and strong proteoglycan staining in the ASC+HA- and SVF+HA-treated groups, whereas rough and fractured surfaces with remarkably heterogeneous cartilage structures were observed in the saline and HA groups (Fig. 4A, 4B). Furthermore, cartilage thickness of the femoral condyle in the high-dose ASC+HA-treated group was also significantly thicker than that observed in the HA and saline groups, although SVF+HA and low-dose ASC+HA treatments resulted in no significance of cartilage thickness compared with that of the HA and saline groups (Fig. 4C). Based on these results, IA injection of autologous ASCs+HA and

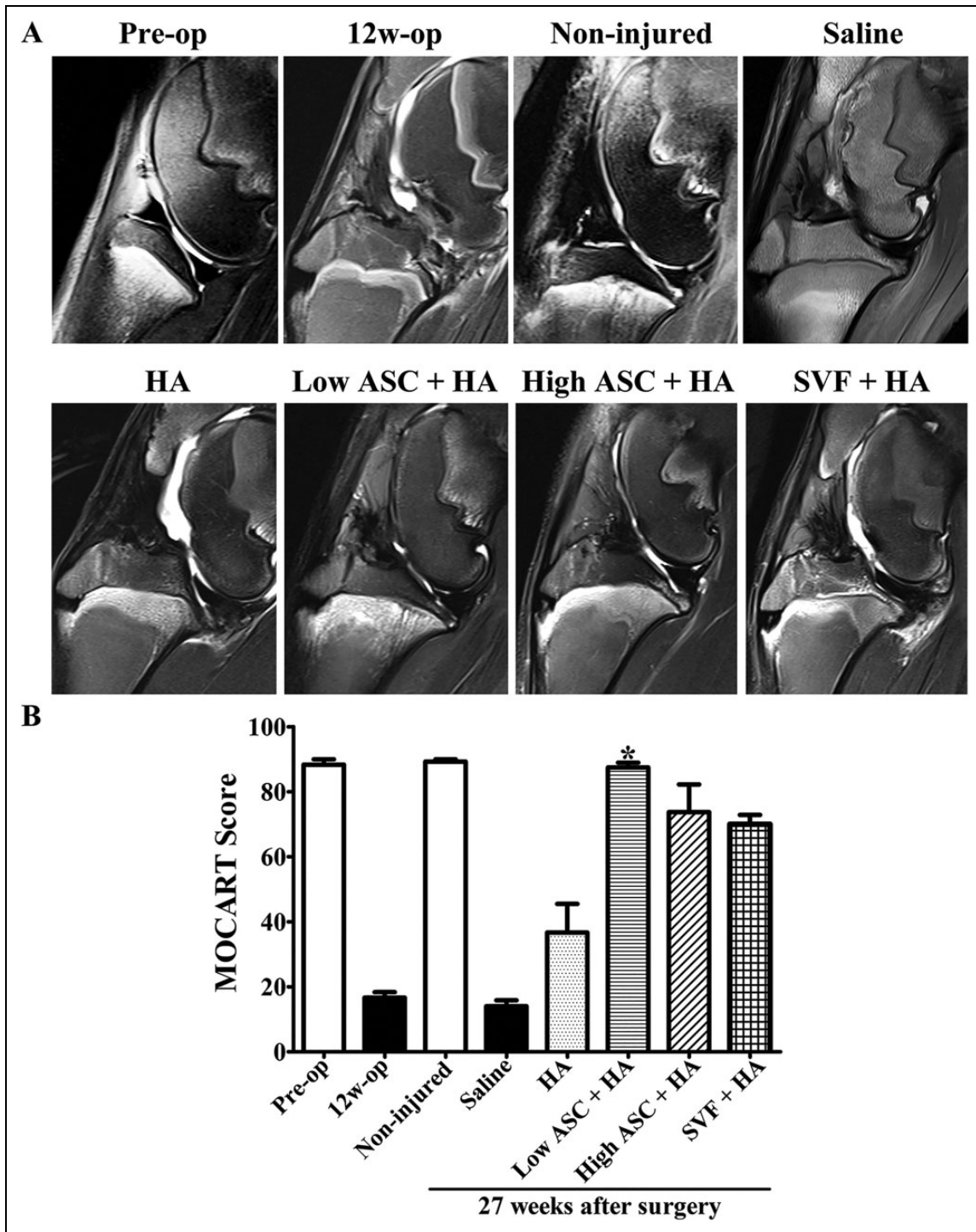


Fig. 2. After OA model was successfully induced, MR imaging indicated the efficacy of autologous low-dose ASC+HA treatment. (A) MRI was performed at pre-operation (pre-op), 12 weeks post-operation (12 w), and 27 weeks post-operation in different treatments (non-injured, saline, HA, low ASC+HA, high ASC+HA, and SVF+HA). In the pre-op and non-injured groups, T2 sequence of 3.0 T MRI showed smooth cartilage layer and clear synovium lining; however, at 12 weeks post-surgery and in the saline and HA groups, the T2 sequence of the MRI exhibited damaged cartilage and hydroptic synovium. ASC+HA and SVF+HA treatments improved cartilage injury, bone marrow lesions of subchondral bone, synovial hydroptic swelling. (B) MOCART scores in low-dose ASC+HA treatment were significantly higher than those in the saline and HA groups. The *P*-values were obtained using a Kruskal–Wallis test and Dunn’s post-test ($*P < 0.05$). Data were collected from three repetitions ($n=3$).

ASC: adipose mesenchymal stem cell; HA: hyaluronic acid; MOCART: magnetic resonance observation of cartilage repair tissue; MRI: magnetic resonance imaging; OA: osteoarthritis; SVF: stromal vascular fraction.

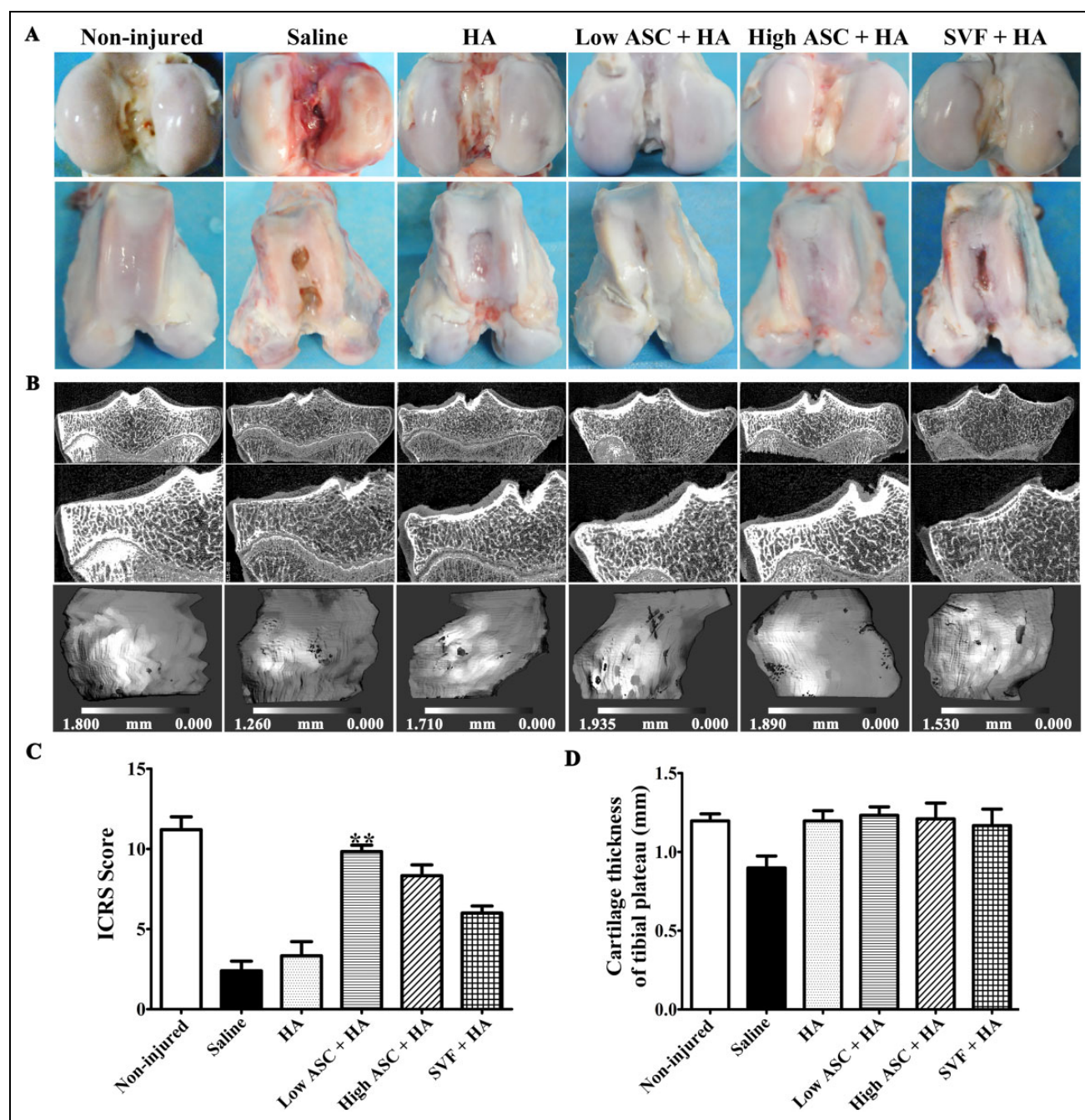


Fig. 3. Macroscopic analysis and μ CT scanning showed autologous ASC+HA exhibited better efficacy than SVF+HA in treating OA. (A) Macroscopy of the articular cartilage surface of femoral condyles at 27 weeks after surgery (12 weeks post second injection) showed more continuous and smoother cartilage layer with no obvious cartilage destruction in the ASC-treated groups than the SVF group. In contrast, visible fissures and cracks to different extent were observed in the saline and HA groups. (B) μ CT evaluations displayed cartilage thickness of tibial plateau at 12 weeks post second injection in each group. After contouring the underlying subchondral bone, three-dimensional images of the medial tibial condyle cartilage surface were reconstructed, respectively. The gray scale represents the thickness of the cartilage at each voxel. Dark areas indicate thinner articular cartilage, while light areas represent thicker articular cartilage. (C) Only low-dose ASC+HA treatment obtained higher ICRS scores of femoral condyles than those of the saline group. (D) Average cartilage thickness of the tibial plateau measured by μ CT images showed that there were no differences in ASC+HA and SVF+HA-treated groups. The *P*-values were obtained using Kruskal–Wallis test and Dunn’s post-test (***P*<0.01). Data were collected from three repetitions (*n*=3). μ CT: micro-computed tomography; ASC: adipose mesenchymal stem cell; HA: hyaluronic acid; ICRS: International Cartilage Research Society; OA: osteoarthritis; SVF: stromal vascular fraction.

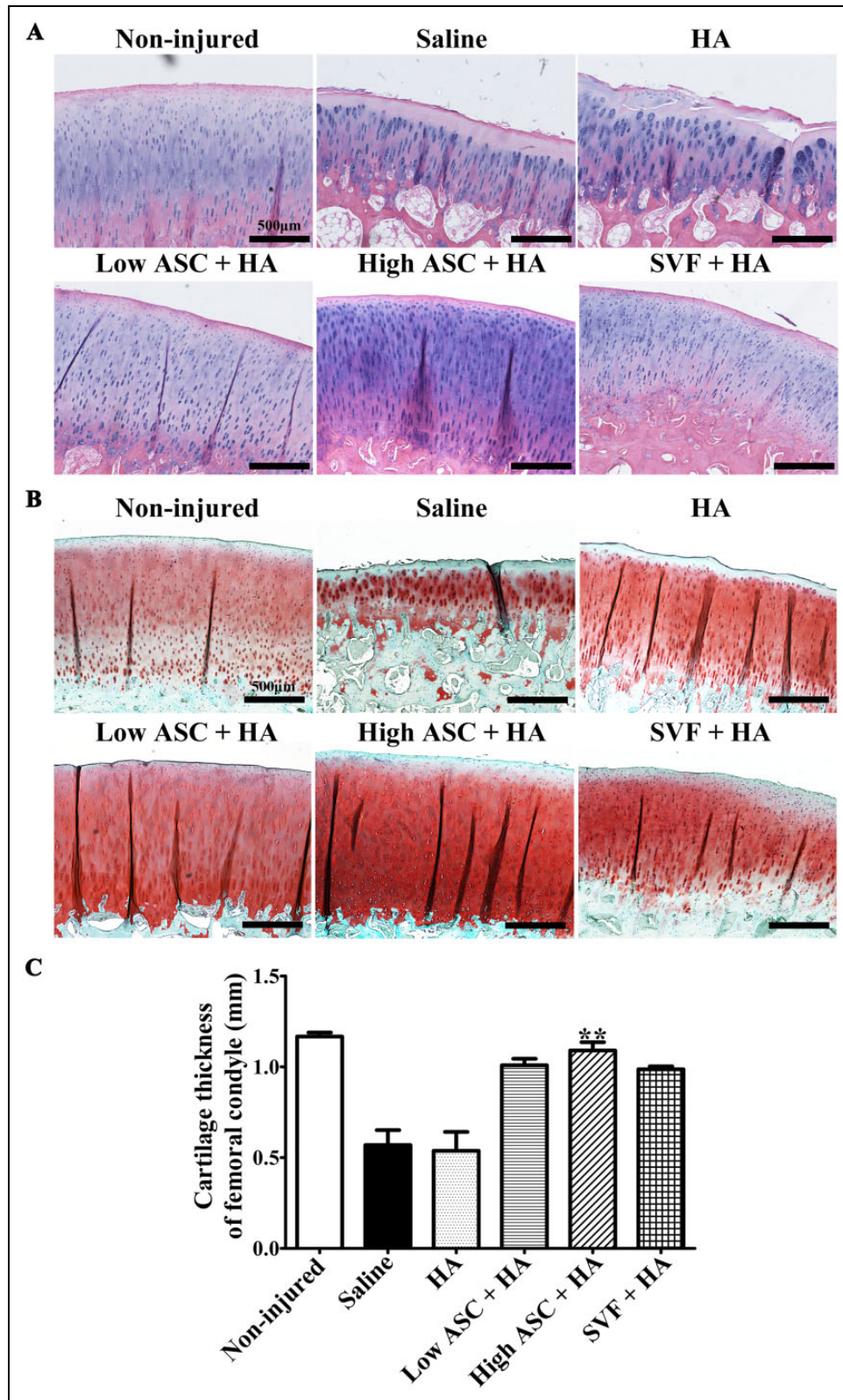


Fig. 4. Histological evaluations showed the efficacy of autologous ASC+HA and SVF+HA treatments. (A) H&E staining and (B) Safranin-O/Fast green staining revealed that autologous ASC+HA and SVF+HA-treated groups presented typical articular cartilage structure and ECM staining with smooth, continuous surface similar to the non-injured group, while the saline and HA groups showed an obvious eroded structure with a rough, cracked surface at 27 weeks post-surgery (12 weeks post second injection). (C) Cartilage thickness of femoral condyles in the high ASC+HA group was significantly thicker than the saline and HA groups. Cartilage thicknesses were calculated from the surface layer (zone I) across transitional stratum (zone II), and radiate stratum (zone III) to calcified cartilage (zone IV). Scale bars indicate 500 μ m. The *P*-values were obtained using Kruskal–Wallis test and Dunn’s post-test (***P*<0.01). Data were collected from three repetitions (*n*=3). ASC: adipose mesenchymal stem cell; ECM: extracellular matrix; H&E: hematoxylin & eosin; HA: hyaluronic acid; SVF: stromal vascular fraction.

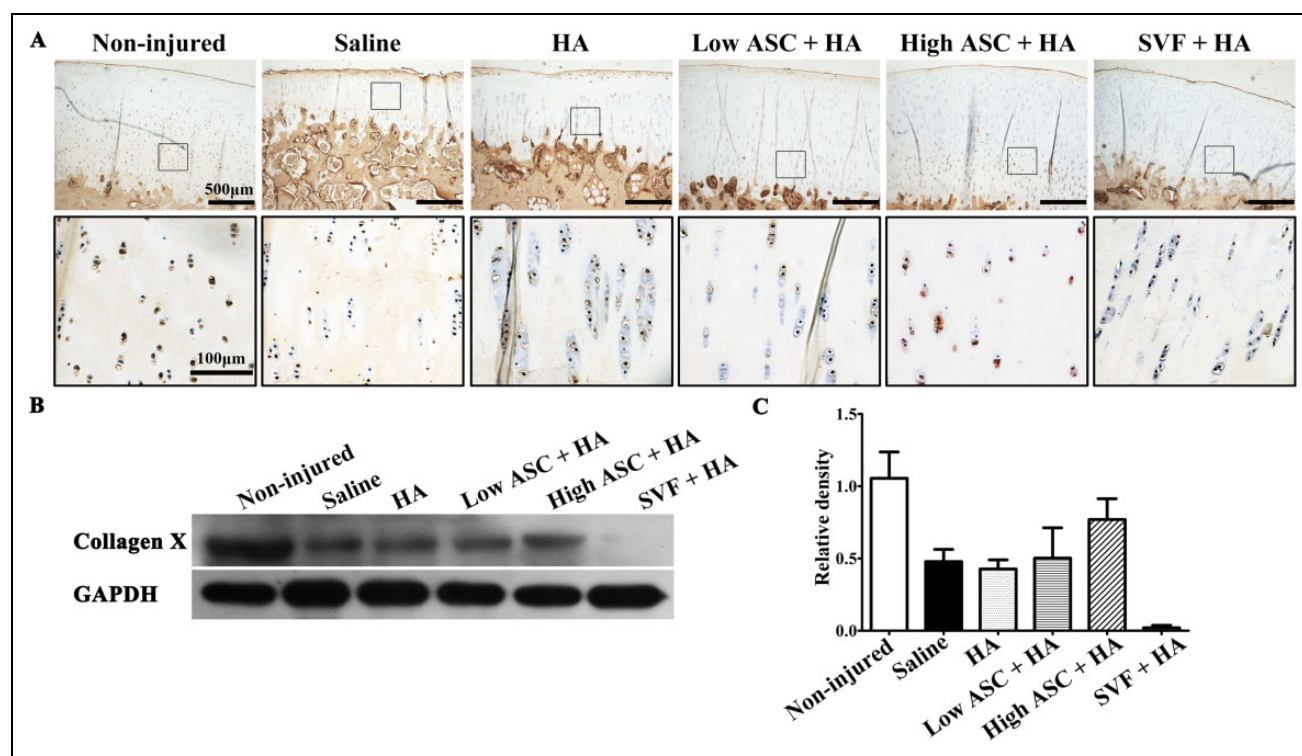


Fig. 5. Type X collagen expression exhibited cartilage quality of autologous ASC+HA and SVF+HA treatments. (A) Immunohistochemistry results showed that hypertrophic chondrocytes expressing collagen X were in alignment at the deep of articular cartilage in the non-injured group. Few collagen-X-positive chondrocytes were observed in the saline and HA-treated groups while high-dose ASC+HA treatment rescued hypertrophic chondrocytes expressing collagen X at the deep area of articular cartilage. It seemed that low-dose ASC+HA treatment showed more collagen-X-positive hypertrophic chondrocytes than that of in SVF+HA treatment. (B, C) Western blot and densitometry analysis results also showed that high- and low-dose ASC+HA treatments expressed collagen X while SVF+HA treatment showed weak expression.

ASC: adipose mesenchymal stem cell; HA: hyaluronic acid; SVF: stromal vascular fraction.

SVF+HA efficiently blocks OA progression, and high-dose ASC+HA treatment achieved better therapeutic efficacy compared with SVF+HA when considering the cartilage matrix and femoral cartilage thickness.

We also examined the expression of type X collagen, a hypertrophic-chondrocyte-specific marker, in the treatment groups. The immunohistochemistry results indicated that hypertrophic chondrocytes expressing collagen X were aligned in the deep articular cartilage in the non-injured group (Fig. 5A). Few collagen-X-positive chondrocytes were observed in the saline and HA treatment groups. In contrast, high-dose ASC+HA treatment rescued hypertrophic chondrocytes expressing collagen X in the deep area of articular cartilage (Fig. 5A). There were greater numbers of collagen-X-positive hypertrophic chondrocytes in the low-dose ASC+HA group than in the SVF+HA group. Furthermore, Western blotting analysis indicated the high- and low-dose ASC+HA groups expressed more collagen X than did the SVF+HA group (Fig. 5B).

In conclusion, these data suggest autologous ASC+HA treatments especially high-dose ASC+HA treatment may promote the regeneration of articular cartilage by increasing cartilage thickness in addition to blocking OA progression.

ASC+HA Treatment exerted Anti-Inflammatory and Trophic Effects

Next, we compared the anti-inflammatory and trophic effects of ASC+HA and SVF+HA treatment. Levels of inflammatory cytokines, including IL-1 β , IL-6, and IL-10, growth factors including TGF- β 1 and IGF-1, and the chemokine SDF-1 were examined in synovial fluid that was collected 12 weeks after the second injection. High-dose ASCs+HA significantly inhibited IL-1 β and IL-6 expression, while the low-dose ASCs+HA and SVF+HA had no significance compared with the saline group. No treatments significantly reduced IL-10 levels, although the high- and low-dose ASC+HA and SVF+HA treatments trended toward reduced IL-10 levels (Fig. 6C). Levels of the chondrogenic agonists TGF- β 1 and IGF-1 were also detected, and no treatments significantly increased TGF- β 1 and IGF-1 levels, although the high- and low-dose ASC+HA and SVF+HA treatments trended toward enhanced TGF- β 1 and IGF-1 levels in synovial fluid (Fig. 6D and E). Additionally, SVF+HA treatment significantly increased SDF-1 levels in the synovial fluid, whereas the low- and high-dose ASC+HA treatments did not affect SDF-1 expression (Fig. 6F).

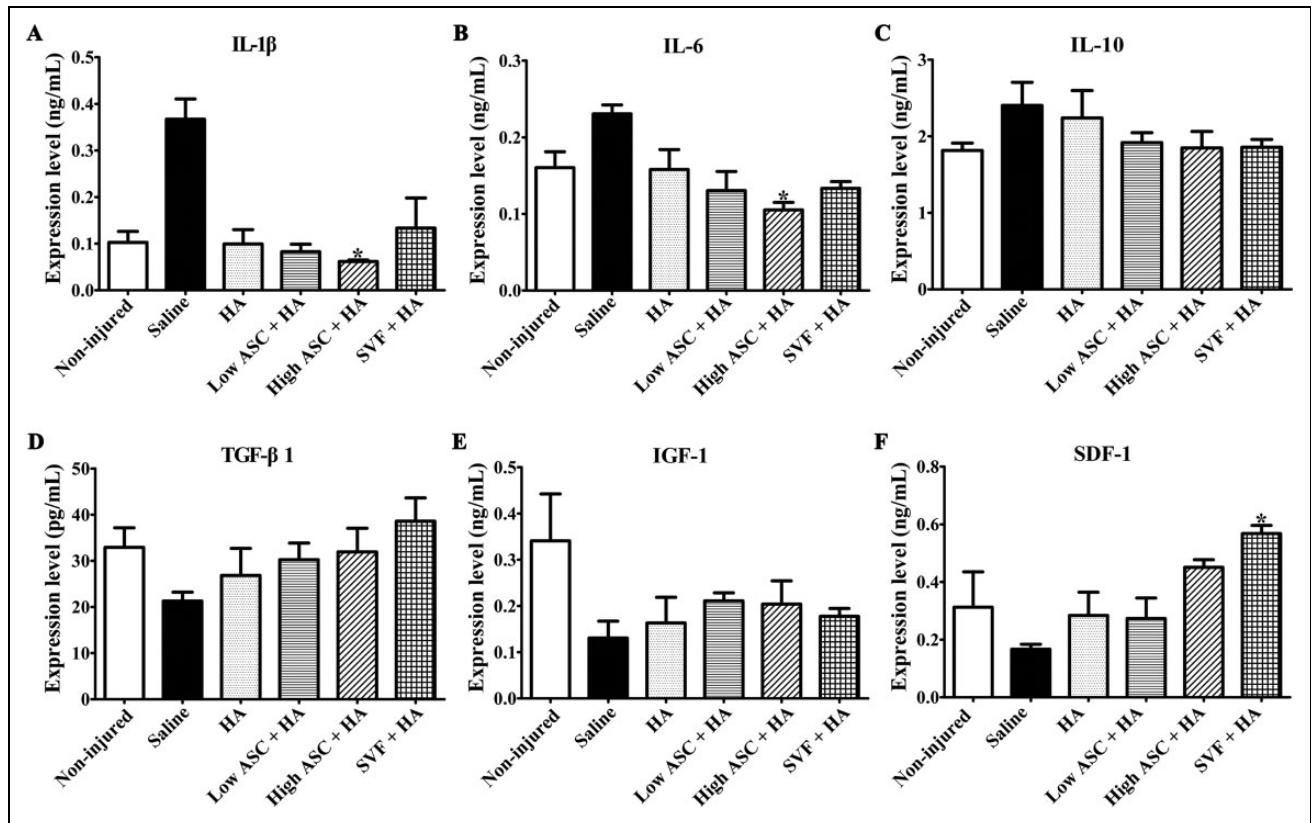


Fig. 6. Autologous ASC+HA treatment displayed anti-inflammatory and trophic effects. ELISA analysis of synovial fluid in each group at 27 weeks after surgery showed only high-dose ASC treatment inhibited (A) IL-1 β expression and (B) IL-6 expression significantly. (C) No treatments significantly reduced IL-10 levels, although the high- and low-dose ASC+HA and SVF+HA treatments trended toward reduced IL-10 levels. No treatments significantly increased (D) TGF- β 1 and (E) IGF-1 levels, although the high- and low-dose ASC+HA and SVF+HA treatments trended toward enhanced TGF- β 1 and IGF-1 levels in synovial fluid. (F) Only SVF+HA treatment significantly increased SDF-1 levels compared with the saline and HA groups. The *P*-values were obtained using Kruskal–Wallis test and Dunn’s post-test (**P*<0.05). Data were collected from three repetitions (*n*=3).

ASC: adipose mesenchymal stem cell; ELISA: enzyme-linked immunosorbent assay; HA: hyaluronic acid; IL: interleukin; IGF: insulin-like growth factor; TGF: transforming growth factor; SDF: stromal cell-derived factor; SVF: stromal vascular fraction.

SPIO Signals Were Present 18 Weeks After Injection and Resided in the Menisci and Marrow Cavities of the Femoral Condyles

To further understand the clearance of autologous ASCs and because high-dose ASC+HA appeared to be more efficacious than low-dose ASC+HA, we explored the persistence of high-dose ASCs labeled with SPIO in the knee joint. After 12 weeks of ACLT and MM, 5×10^7 (high-dose) SPIO-labeled autologous ASCs combined with HA were injected into the OA joint. SPIO signals were detected in the synovium, suprapatellar bursa, and popliteal fossa by MRI until 18 weeks after the injection (30 weeks after ACLT and MM) (Fig. 7A). Prussian blue staining was also used to evaluate the localization of SPIO-labeled cells, and SPIO signals were primarily observed at the edge of the lateral meniscus but not in the articular cartilage at 2 weeks post-injection (14 weeks after ACLT and MM), (Fig. 7B). Moreover, safranin-O/fast green staining confirmed the

presence of SPIO signals in the collagen-I-positive meniscus (Fig. 7B). At 18 weeks post-injection (30 weeks after ACLT and MM), CD68-negative SPIO signals were detected in the marrow cavities of the medial femoral condyles (Fig. 7B), indicating the SPIO particles were not phagocytosed by macrophages.

Discussion

Previous studies from our laboratory revealed the engraftment of xenogeneic human ASCs into rabbit and rat articular cartilage and the inhibition of inflammatory factor levels in synovial fluid^{18,19}; synovial inflammation is a trigger for OA symptoms, and soluble inflammatory factors increase cartilage damage^{31,32}. Recently, a proof-of-concept clinical trial treated OA with $1-10 \times 10^7$ autologous ASC+HA and demonstrated improved WOMAC scores at 6 months after injection in the 10×10^7 dose group, and arthroscopy and histological assessments showed substantial, thick, hyaline-

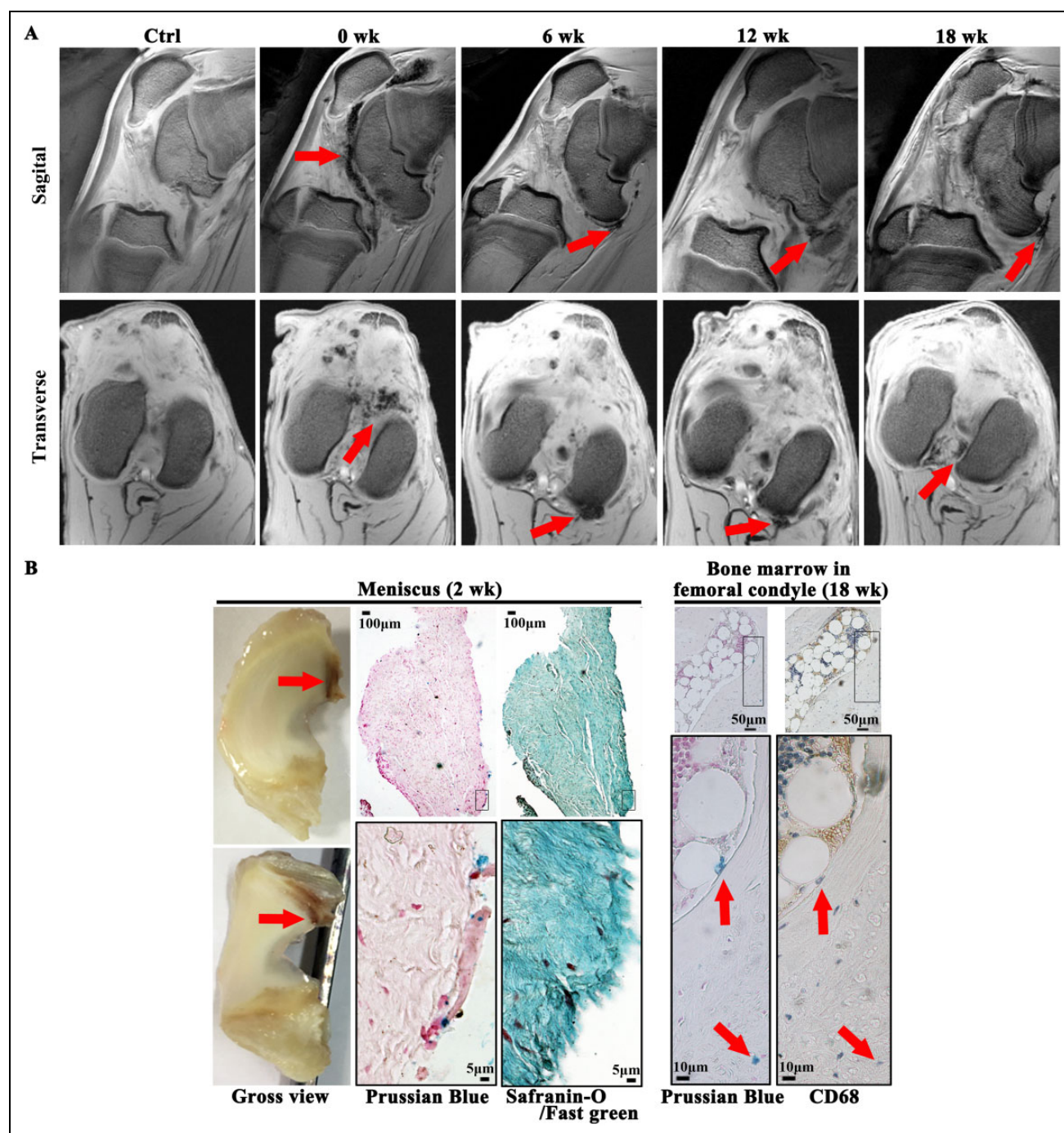


Fig. 7. Signal of SPIO-labeled autologous ASC+HA lasted 18 weeks after injection and SPIO signals were found in meniscus and bone marrow of femoral condyles. (A) T2* sequence of 3.0 T MRI showed SPIO signals mainly located in patellar capsule and joint cavity right after injection (at week 12 of surgery) and then moved to caudal synovial lining lasting for 18 weeks after injection (30 weeks post-surgery) coinciding with efficacy of autologous ASCs observed. (B) At 2 weeks post-injection Prussian blue staining revealed the signals of SPIO were mainly observed at the edge of lateral meniscus and safranin-O/fast green staining confirmed that the tissue which SPIO signals resided was collagen-I-positive meniscus. At 18 weeks post-injection (30 weeks after ACLT and medial meniscectomy), CD68-negative SPIO signals were detected in the marrow cavities of the medial femoral condyles, indicating the SPIO particles were not phagocytosed by macrophages. ACLT: anterior cruciate ligament transection; ASC: adipose mesenchymal stem cell; HA: hyaluronic acid; MRI: magnetic resonance imaging; SPIO: superparamagnetic iron oxide particle; SVF: stromal vascular fraction.

like cartilage regeneration, indicating the feasibility of stem cell therapy for OA⁹. SVF was first injected with HA and PRP into the knee joints of OA patients in 2011, resulting in

decreased VAS pain scores, ameliorated FRI joint function, and improved regeneration of the articular cartilage and subchondral bone⁶. Moreover, in another case series, SVF was

injected after arthroscopic debridement and lavage into 37 OA knees with lesion sizes of $5.4 \pm 2.9 \text{ cm}^2$, and follow up at 26.5 months (24–34 months) revealed significant improvement of both the mean IKDC (International Knee Documentation Committee) and Tegner activity scale scores. A high body mass index (BMI) ($\geq 27.5 \text{ kg/m}^2$) and a large lesion size ($\geq 5.4 \text{ cm}^2$) were significant predictors of poor clinical and arthroscopic outcomes⁸. Most recently, micro-fracture in the presence and absence of SVF and PRP injection were also investigated to treat grade 2 or 3 Lawrence scale OA patients clinically. A mixture of SVF (5×10^7) and activated PRP was injected after arthroscopic micro-fracture into 15 patients (58.60 ± 6.48 years old), while another 15 OA patients (58.20 ± 5.71 years old) received only micro-fracture as a control. During follow up, WOMAC scores in both groups significantly decreased compared with the baseline at 6 and 12 months after treatment; however, at 18 months after treatment, WOMAC scores in the micro-fracture group deteriorated and were not significantly different compared with the baseline, while WOMAC scores in the micro-fracture + SVF group improved continuously³³. However, one of the main disadvantages of using autologous SVF in OA patients is the lack of availability of randomized controlled studies; only case reports or cohort studies have been conducted. Despite the beneficial results published by these case reports and cohort studies, further investigation is necessary to accept SVF as a standard cell therapy treatment for OA. Additionally, both ASCs and SVF are heterogeneous cell populations, and both have shown efficacy for the treatment of OA, but it is not clear which is more efficacious. In this study, two injections of both autologous ASC+HA and SVF+HA improved MOCART scores of OA animals to the same extent (Fig. 2). Macroscopic and histological evaluations of the same treatment dose (1×10^7) indicated autologous ASC+HA resulted in better cartilage uniformity than that observed in the SVF+HA group, although both autologous ASC+HA and SVF+HA treatments demonstrated efficacy (Figs. 3 and 4).

SVF contains colony-forming unit fibroblasts (CFU-Fs) at a frequency of 1–10% and expresses the stromal cell-associated markers CD13, CD29, CD44, CD63, CD73, CD90, CD 105, and CD146, although these stromal markers are expressed at very low levels^{12,34,35}. A CFU-F assay was performed to evaluate the frequency of mesenchymal progenitors in SVF. Positive CFU-F and stromal cell-associated characteristics may explain why SVF showed efficacy in blocking OA in the current study; although it is not a homogeneous cell population, SVF contains mesenchymal stromal cells, and its final mesenchymal stromal population composition has varied considerably in different studies due to differing fluorescent-activated cell sorting techniques, cellular extraction steps, and adipose tissues extracted from different regions of the body³⁴. Furthermore, the presence of mesenchymal stromal cell populations may also explain why SVF trended toward increased TGF- β 1 levels in synovial fluid. In contrast, ASCs are less heterogeneous than SVF

cells because they expand from an adherent cell population and contain CFU-F at a frequency of $1:3 \pm 2$ at passage 4, thus demonstrating greater numbers of mesenchymal progenitors and superior multipotency¹². This might explain why the efficacy of ASC+HA was superior to that of SVF+HA in the current study. The current study not only undertook macroscopic and histological analyses of articular cartilage but also investigated synovial inflammation. Our results were consistent with previous investigations in which SVF demonstrated less potency to decrease IL-1 β and IL-6 levels (Fig. 6A and B), which in turn promoted cartilage catabolic responses³⁶. SDF-1 plays an important role in OA progression: SDF-1 secreted by synoviocytes combines with the C-X-C chemokine receptor type 4 (CXCR4) receptor on the chondrocyte membrane and activates the Erk and P38 mitogen-activated protein kinase signaling pathway to induce matrix metalloproteinase (MMP) expression and degradation of the extracellular matrix (ECM)^{37,38}. In our study, SVF+HA increased SDF-1 secretion (Fig. 6F), whereas ASC+HA treatments did not, suggesting the superior efficacy of ASC+HA for the treatment of OA.

Recently, the efficacies of BM-MSCs and SVF for the treatment of OA were investigated, showing no significant effects³⁹. However, the primary concern regarding this study is the differing dosages of SVF and BM-MSCs. Horses ($n=8$) in the SVF group received a total of 1.63×10^7 nucleated cells, which is equivalent to 0.2×10^7 SVF cells per OA horse, whereas horses ($n=8$) in the BM-MSC group received a total of 1.05×10^7 BM-MSCs, which is equivalent to 0.13×10^7 BM-MSCs per OA horse. Another concern is the application of only one small dose ($0.13\text{--}0.2 \times 10^7$ BM-MSCs or SVF cells): efficacy may not have been observed because one dose might not be sufficient to treat a skeletally mature horse with OA. Additionally, the follow-up period may have been too short to observe efficacy. In our study, the same dose (1×10^7 cells) of ASC and SVF was applied to treat OA sheep. Moreover, two large doses were administered due to animal body weight consideration. OA was induced in 30 kg sheep, and a second dose (1×10^7 cells) was given 3 weeks after the first to ensure efficacy. Finally, we followed up for 12 weeks (15 weeks after the first injection) rather than 8 weeks to evaluate efficacy. In summary, larger doses, repeated injections, lower animal body weights, and a longer follow-up period may explain why efficacy was observed in the current study.

From a pharmacological perspective, it is very important to understand the pharmacokinetic/pharmacodynamic relationship for a cell therapy ‘drug’. Since SVF is usually used when fresh, and the labeling protocol often requires overnight culture, co-culturing SVF with a labeling reagent overnight would damage cells in the hematopoietic subgroup of SVF, resulting in labeling difficulties. Therefore, in the current study, we labeled only autologous ASCs to detect persistence. Moreover, the SVF yield from adipose tissue made it difficult to deliver 5×10^7 cells per dose. The efficacy of high-dose ASC+HA appeared superior to that of low-dose

ASC+HA. Thus, high-dose ASCs were labeled in combination with HA to evaluate their lifespan after IA injection. We labeled the ASCs with SPIO, a 35-nm non-transfection-based fluorescent iron oxide nanoparticle, traced their localization after joint injection in a large animal model of OA and observed the presence of SPIO signals for 18 weeks by MRI (30 weeks after ACLT and MM surgery), which included the efficacy assessment time point at week 12. Interestingly, histological examination detected signals only at the surface of the lateral menisci and bone marrow cavities of the femoral condyles (Fig. 7B). However, we can only exclude the phagocytosis by macrophages but the SPIO positive cells might not be the injected ASCs. Further investigation at multiple timepoints should be conducted to survey various tissues and clarify whether autologous ASC engraftment to cartilage is an efficacy requirement.

There are certain limitations to this study. For example, simultaneously acquiring a large group of nearly 40 adult sheep was difficult. Thus, we used adolescent sheep to explore the efficacy of cell therapy. However, OA primarily occurred in adults, although a previous study demonstrated the synovial homogeneity of immature and adult sheep with respect to the consistently low expression of the inflammatory factors TNF- α , IL-1 β , and IL-6, which are essential for the initiation and development of OA⁴⁰. Furthermore, the current study prepared autologous sheep ASCs and SVF to demonstrate the effective blockade of cartilage destruction and promotion of cartilage regeneration in a sheep OA model following repeated injections of bona fide autologous ASCs and SVF. Whereas SVF is often used fresh, cryopreserved SVF and ASCs were used in the current study for the second injection at week 15 because it was very difficult to perform a third surgery to isolate adipose tissue from each sheep. Further studies are necessary to address this problem. Additionally, this issue reveals the limitations of SVF for clinical applications, while ASCs may be passaged to expand their population. Another limitation is that we mainly focus on cartilage changes in the current study but OA is an organ disease with cartilage degradation, subchondral bone sclerosis, ligament retrogression, synovium hyperplasia, and joint capsule hypertrophy². Although MRI exhibited ASC+HA-improved hydropic synovium and bone marrow lesions of subchondral bone (Fig. 2), the detailed pathological assays of subchondral bone, ligament, synovium, and joint capsule were not exhibited. Further investigations should be performed to address all these limitations.

Conclusions

The current study demonstrated significantly improved MOCART and ICRS scores following treatment with low-dose ASCs+HA compared with SVF+HA treatment. Although no differences were exhibited in terms of cartilage thickness of the tibial plateau (Fig. 3D), high-dose ASC+HA treatment resulted in a significant increase in cartilage thickness of the femoral epicondyle, while low-dose ASC+HA

and SVF+HA treatments showed no differences in improving cartilage thickness of the femoral epicondyle. Based on the synovial fluid data, only high-dose ASC+HA treatment inhibited IL-1 β and IL-6 expressions. Furthermore, only SVF+HA treatment enhanced SDF-1 expression in synovial fluid. In conclusion, IA injection of autologous ASC+HA may result in better efficacy than autologous SVF+HA in blocking OA progression and promoting cartilage regeneration, and autologous ASCs (5×10^7 cells) may survive for at least 18 weeks after IA injection.

Acknowledgments

We would like to thank Dr Wei Liu and Junming Lu (National Tissue Engineering Center of China) for technical assistance and scientific advice.

Authors Contribution

Xiaoteng Lv, Jiyin He, Xue Zhang, Xuan Luo contributed equally.

Ethical Approval

All animal experimental protocols were approved by the Ethics Committee of Shanghai Jiao Tong University School of Medicine.

Statement of Human and Animal Rights

All following experiments and animal rights were complied with relevant guidelines and regulations.

Statement of Informed Consent

There are no human subjects in this article and informed consent is not applicable.

Declaration of Conflicting Interests

The authors declared the following potential conflicts of interest with respect to the research, authorship, and/or publication of this article: Xiaoteng Lv, Zhongwei Sun, Victor Liu, and Li Zhang are current employees and shareholders of Cellular Biomedicine Group (Nasdaq: CBMG). Other authors declare no competing financial interests.

Funding

The authors disclosed receipt of the following financial support for the research, authorship, and/or publication of this article: The current study was supported by Shanghai Innovation Funding (1402H294300) sponsored by the Science and Technology Commission of Shanghai Municipality (CN) to Dr Wen Wang. The funding body had no role in the design of the study and collection, analysis, and interpretation of data, or in writing the manuscript.

References

1. Kraus VB, Blanco FJ, Englund M, Karsdal MA, Lohmander LS. Call for standardized definitions of osteoarthritis and risk stratification for clinical trials and clinical use. *Osteoarthritis Cartilage*. 2015;23(8):1233–1241.
2. Loeser RF, Goldring SR, Scanzello CR, Goldring MB. Osteoarthritis: a disease of the joint as an organ. *Arthritis Rheum*. 2012;64(6):1697–1707.

3. Reginster JY, Reiter-Niesert S, Bruyere O, Berenbaum F, Brandi ML, Branco J, Devogelaer JP, Herrero-Beaumont G, Kanis J, Maggi S and others. Recommendations for an update of the 2010 European regulatory guideline on clinical investigation of medicinal products used in the treatment of osteoarthritis and reflections about related clinically relevant outcomes: expert consensus statement. *Osteoarthritis Cartilage*. 2015;23(12):2086–93.
4. Brown GA. AAOS clinical practice guideline: treatment of osteoarthritis of the knee: evidence-based guideline 2nd edition. *J Am Acad Orthop Surg*. 2013;21(9):577–579.
5. Glyn-Jones S, Palmer AJ, Agricola R, Price AJ, Vincent TL, Weinans H, Carr AJ. Osteoarthritis. *Lancet*. 2015;386(9991):376–387.
6. Pak J. Regeneration of human bones in hip osteonecrosis and human cartilage in knee osteoarthritis with autologous adipose-tissue-derived stem cells: a case series. *J Med Case Rep*. 2011; 5:296.
7. Koh YG, Jo SB, Kwon OR, Suh DS, Lee SW, Park SH, Choi YJ. Mesenchymal stem cell injections improve symptoms of knee osteoarthritis. *Arthroscopy*. 2013;29(4):748–755.
8. Koh YG, Choi YJ, Kwon OR, Kim YS. Second-Look Arthroscopic Evaluation of Cartilage Lesions After Mesenchymal Stem Cell Implantation in Osteoarthritic Knees. *Am J Sports Med*. 2014;42(7):1628–1637.
9. Jo CH, Lee YG, Shin WH, Kim H, Chai JW, Jeong EC, Kim JE, Shim H, Shin JS, Shin IS and others. Intra-articular injection of mesenchymal stem cells for the treatment of osteoarthritis of the knee: a proof-of-concept clinical trial. *Stem Cells*. 2014;32(5):1254–1266.
10. Kim YS, Choi YJ, Suh DS, Heo DB, Kim YI, Ryu JS, Koh YG. Mesenchymal stem cell implantation in osteoarthritic knees: is fibrin glue effective as a scaffold? *Am J Sports Med*. 2015; 43(1):176–185.
11. McIntosh K, Zvonic S, Garrett S, Mitchell JB, Floyd ZE, Hammill L, Kloster A, Di Halvorsen Y, Ting JP, Storms RW and others. The immunogenicity of human adipose-derived cells: temporal changes in vitro. *Stem Cells*. 2006;24(5):1246–53.
12. Mitchell JB, McIntosh K, Zvonic S, Garrett S, Floyd ZE, Kloster A, Di Halvorsen Y, Storms RW, Goh B, Kilroy G and others. Immunophenotype of human adipose-derived cells: temporal changes in stromal-associated and stem cell-associated markers. *Stem Cells*. 2006;24(2):376–85.
13. Han J, Koh YJ, Moon HR, Ryoo HG, Cho CH, Kim I, Koh GY. Adipose tissue is an extramedullary reservoir for functional hematopoietic stem and progenitor cells. *Blood*. 2010;115(5): 957–964.
14. Cawthorn WP, Scheller EL, MacDougald OA. Adipose tissue stem cells: the great WAT hope. *Trends Endocrinol Metab*. 2012;23(6):270–277.
15. Desando G, Cavallo C, Sartoni F, Martini L, Parrilli A, Veronesi F, Fini M, Giardino R, Facchini A, Grigolo B. Intra-articular delivery of adipose-derived stromal cells attenuates osteoarthritis progression in an experimental rabbit model. *Arthritis Res Ther*. 2013;15(1):R22.
16. Yanez R, Lamana ML, Garcia-Castro J, Colmenero I, Ramirez M, Bueren JA. Adipose tissue-derived mesenchymal stem cells have in vivo immunosuppressive properties applicable for the control of the graft-versus-host disease. *Stem Cells*. 2006; 24(11):2582–2591.
17. Ivanova-Todorova E, Bochev I, Mourdjeva M, Dimitrov R, Bukarev D, Kyurkchiev S, Tivchev P, Altunkova I, Kyurkchiev DS. Adipose tissue-derived mesenchymal stem cells are more potent suppressors of dendritic cells differentiation compared to bone marrow-derived mesenchymal stem cells. *Immunol Lett*. 2009;126(1–2):37–42.
18. Wang W, He N, Feng C, Liu V, Zhang L, Wang F, He J, Zhu T, Wang S, Qiao W, Li S, Zhou G, Zhang L, Dai C, Cao W. Human adipose-derived mesenchymal progenitor cells engraft into rabbit articular cartilage. *Int J Mol Sci*. 2015;16(6): 12076–91.
19. Li M, Luo X, Lv X, Liu V, Zhao G, Zhang X, Cao W, Wang R, Wang W. In vivo human adipose-derived mesenchymal stem cell tracking after intra-articular delivery in a rat osteoarthritis model. *Stem Cell Res Ther*. 2016;7(1):160.
20. Bendele AM. Animal models of osteoarthritis. *J Musculoskelet Neuronal Interact*. 2001;1(4):363–376.
21. Murphy JM, Fink DJ, Hunziker EB, Barry FP. Stem cell therapy in a caprine model of osteoarthritis. *Arthritis Rheum*. 2003; 48(12):3464–3474.
22. Bayne K, Ramachandra GS, Rivera EA, Wang J. The evolution of animal welfare and the 3Rs in Brazil, China, and India. *J Am Assoc Lab Anim Sci*. 2015;54(2):181–191.
23. Zuk PA, Zhu M, Mizuno H, Huang J, Futrell JW, Katz AJ, Benhaim P, Lorenz HP, Hedrick MH. Multilineage cells from human adipose tissue: implications for cell-based therapies. *Tissue Eng*. 2001;7(2):211–228.
24. Zuk PA, Zhu M, Ashjian P, De Ugarte DA, Huang JI, Mizuno H, Alfonso ZC, Fraser JK, Benhaim P, Hedrick MH. Human adipose tissue is a source of multipotent stem cells. *Mol Biol Cell*. 2002;13(12):4279–4795.
25. Feng C, Luo X, He N, Xia H, Lv X, Zhang X, Li D, Wang F, He J, Zhang L, Lin X, Lin L, Yin H, He J, Wang J, Cao W, Wang R, Zhou G, Wang W. Efficacy and persistence of allogeneic adipose-derived mesenchymal stem cells combined with hyaluronic acid in osteoarthritis after intra-articular injection in a sheep model. *Tissue Eng Part A*. 2018;24(3–4):219–233.
26. Marlovits S, Striessnig G, Resinger CT, Aldrian SM, Vecsei V, Imhof H, Trattnig S. Definition of pertinent parameters for the evaluation of articular cartilage repair tissue with high-resolution magnetic resonance imaging. *Eur J Radiol*. 2004; 52(3):310–319.
27. Little CB, Smith MM, Cake MA, Read RA, Murphy MJ, Barry FP. The OARSI histopathology initiative - recommendations for histological assessments of osteoarthritis in sheep and goats. *Osteoarthritis Cartilage*. 2010;18(Suppl. 3): S80–S92.
28. Brittberg M, Winalski CS. Evaluation of cartilage injuries and repair. *J Bone Joint Surg Am*. 2003;85(A Suppl. 2):58–69.
29. Kotwal N, Li J, Sandy J, Plaas A, Sumner DR. Initial application of EPIC-muCT to assess mouse articular cartilage

- morphology and composition: effects of aging and treadmill running. *Osteoarthritis Cartilage*. 2012;20(8):887–895.
30. Pastoureau P, Leduc S, Chomel A, De Ceuninck F. Quantitative assessment of articular cartilage and subchondral bone histology in the meniscectomized guinea pig model of osteoarthritis. *Osteoarthritis Cartilage*. 2003;11(6):412–423.
 31. Sellam J, Berenbaum F. The role of synovitis in pathophysiology and clinical symptoms of osteoarthritis. *Nat Rev Rheumatol*. 2010;6(11):625–635.
 32. Scanzello CR, McKeon B, Swaim BH, DiCarlo E, Asomugha EU, Kanda V, Nair A, Lee DM, Richmond JC, Katz JN, Crow MK, Goldring SR. Synovial inflammation in patients undergoing arthroscopic meniscectomy: molecular characterization and relationship to symptoms. *Arthritis Rheum*. 2011;63(2):391–400.
 33. Nguyen PD, Tran TD, Nguyen HT, Vu HT, Le PT, Phan NL, Vu NB, Phan NK, Van Pham P. Comparative clinical observation of arthroscopic microfracture in the presence and absence of a stromal vascular fraction injection for osteoarthritis. *Stem Cells Transl Med*. 2017;6(1):187–195.
 34. Astori G, Vignati F, Bardelli S, Tubio M, Gola M, Albertini V, Bambi F, Scali G, Castelli D, Rasini V, Soldati G, Moccetti T. “In vitro” and multicolor phenotypic characterization of cell subpopulations identified in fresh human adipose tissue stromal vascular fraction and in the derived mesenchymal stem cells. *J Transl Med*. 2007;5:55.
 35. Bourin P, Bunnell BA, Casteilla L, Dominici M, Katz AJ, March KL, Redl H, Rubin JP, Yoshimura K, Gimble JM. Stromal cells from the adipose tissue-derived stromal vascular fraction and culture expanded adipose tissue-derived stromal/stem cells: a joint statement of the International Federation for Adipose Therapeutics and Science (IFATS) and the International Society for Cellular Therapy (ISCT). *Cytotherapy*. 2013;15(6):641–648.
 36. Catterall JB, Stabler TV, Flannery CR, Kraus VB. Changes in serum and synovial fluid biomarkers after acute injury (NCT00332254). *Arthritis Res Ther*. 2010;12(6):R229.
 37. Santiago B, Baleux F, Palao G, Gutierrez-Canas I, Ramirez JC, Arenzana-Seisdedos F, Pablos JL. CXCL12 is displayed by rheumatoid endothelial cells through its basic amino-terminal motif on heparan sulfate proteoglycans. *Arthritis Res Ther*. 2006;8(2):R43.
 38. Chiu YC, Fong YC, Lai CH, Hung CH, Hsu HC, Lee TS, Yang RS, Fu WM, Tang CH. Thrombin-induced IL-6 production in human synovial fibroblasts is mediated by PAR1, phospholipase C, protein kinase C alpha, c-Src, NF-kappa B and p300 pathway. *Mol Immunol*. 2008;45(6):1587–1599.
 39. Frisbie DD, Lu Y, Kawcak CE, DiCarlo EF, Binette F, McIlwraith CW. In vivo evaluation of autologous cartilage fragment-loaded scaffolds implanted into equine articular defects and compared with autologous chondrocyte implantation. *Am J Sports Med*. 2009;37(Suppl. 1):71S–80S.
 40. Solbak N, Achari Y, Chung M, Shrive NG, Hart DA, Frank CB. Normal sheep synovium has similar appearances and constitutive expression of inflammatory cytokines within and between knee joints: a baseline histological and molecular analysis. *Connect Tissue Res*. 2014;55(2):156–163.